Gravothermal catastrophe in anisotropic systems (*)

M. MAGLIOCCHETTI ([1])([3]), G. PUCACCO ([2])([3]) and E. VESPERINI ([4])

([1]) *Dipartimento di Fisica, Università di Roma I "La Sapienza" P.le A. Moro 2, I-00185 Roma, Italy*
([2]) *Dipartimento di Fisica, Università di Roma II "Tor Vergata" Via della Ricerca Scientifica 1, I-00133 Roma, Italy*
([3]) *ICRA, International Center for Relativistic Astrophysics - Roma, Italy*
([4]) *Scuola Normale Superiore di Pisa - P.zza Cavalieri 7, I-50126 Pisa, Italy*

(ricevuto il 30 Luglio 1996)

Summary. — In this paper we investigate the gravothermal instability of spherical stellar systems endowed with an anisotropic velocity distribution, focussing our attention on the connections between the conditions for the onset of the gravothermal instability and the amount of anisotropy globally present inside the system. The investigation has been carried out by the *method of linear series*, introduced by Poincaré in 1885 (*Acta Math.*, **7** (1885) 259); by studying the influence of the internal kinematics on the global features of these models we have found out that a greater number of radial orbits affect the process in a dramatic way, in the sense that the stronger is the anisotropy the sooner a system looses stability (where the word "sooner" means for smaller central potentials). As a final step, we evaluated the stability of these systems with respect to the *radial-orbit instability*, a dynamical process occurring because of the anisotropy that leads to a modification of their internal structure, and such results have been compared with those coming from the former analysis, to exclude the presence of this second phenomenon during the study of the gravothermal catastrophe.

PACS 04.20 – Classical general relativity.
PACS 98.20.Gm – Globar clusters in the Milky Way.
PACS 98.20.Jp – Globar clusters in external galaxies.
PACS 01.30.Cc – Conference proceedings.

1. – A brief review on the problem of the gravothermal instability

Let us consider a self-gravitating system and define its temperature T by means of

$$\frac{1}{2} m \langle v(r) \rangle^2 = \frac{3}{2} \kappa T(r) , \tag{1}$$

(*) Paper presented at the Fourth Italian-Korean Meeting on Relativistic Astrophysics, Rome-Gran Sasso-Pescara, July 9-15, 1995.

where m is the mass of a single star composing the system, $\langle v(r) \rangle$ is the rms velocity and κ is the Boltzmann constant. For a system composed by N stars of the same mass, the kinetic energy K is given by

$$K = \frac{3}{2} N \kappa \overline{T} \tag{2}$$

with $\overline{T}$ defined as

$$\overline{T} = \frac{\int \varrho(\mathbf{r})\, T(\mathbf{r})\, \mathrm{d}\mathbf{r}}{\int \varrho(\mathbf{r})\, \mathrm{d}\mathbf{r}} ,$$

where $\varrho(\mathbf{r})$ is the density. If this system is isolated and in thermodynamic equilibrium, from the virial theorem in the absence of boundary pressure $K = -E$ follows, with E the total energy of the system, and where we used the conservation energy law. This last statement and eq. (1) imply

$$E = -\frac{3}{2} N \kappa \overline{T} ; \tag{3}$$

therefore we can conclude that a self-gravitating system is featured by having a specific heat $C = \frac{\mathrm{d}E}{\mathrm{d}\overline{T}}$ which is always negative.

Now let us suppose to enclose a self-gravitating, isothermal system into a spherical box endowed with isolating and reflecting walls, and imagine also to divide it into two subsystems, the first one mainly held together by its gravitation (*core*) while the second one, less dense and therefore less subjected to self-gravitation, mainly held together by the walls of the box. This situation implies that the core has a negative specific heat $C_{\mathrm{c}} < 0$, while for the halo we have $C_{\mathrm{h}} > 0$ (see [1]).

Let r_{i} be the initial radius of the box, with $r_{\mathrm{i}} < r_{\mathrm{c}}$, where $r_{\mathrm{c}} = -0.335 GM^2/E$ is the critical radius whose value was first obtained by Antonov [2]. Imagine now to remove suddenly the walls of the box: the system will expand until it settles into a configuration with $r_{\mathrm{f}} > r_{\mathrm{i}}$; this expansion will happen without loosing energy because the system has always been supposed to be isolated, and therefore the whole result will be an adiabatic cooling, even if not all its parts will cool in the same way. In fact the nucleus, being more bound, will cool and will expand less than the halo: as a consequence of that, there will be the onset of a temperature gradient and of a heating flux from the inner regions of the system to the outer ones; because of the difference between the signs of the specific heats both the subsystems will heat up, the core loosing energy and the halo gaining it. Now we can face two situations:

1) If the specific heat of the halo is smaller than the absolute value of the specific heat of the core its temperature will grow faster than the one of the core until we reach the situation $T_{\mathrm{H}} > T_{\mathrm{C}}$; in this case the flux stops and it is possible to reach an equilibrium configuration. This happens whenever $r_{\mathrm{f}} < r_{\mathrm{c}}$.

2) If the halo is wide enough ($r_{\mathrm{f}} > r_{\mathrm{c}}$) its specific heat, being an extensive quantity, will be greater than the absolute value of the specific heat of the core; in this situation the nucleus will heat up more quickly than the halo, and while heating it will transfer energy to the outer parts and will contract always more. No equilibrium situation is possible; this process will happen irreversibly and always faster. The final result will be

a system composed by a denser and denser and smaller and smaller nucleus surrounded by a growing halo. This phenomenon is called *gravothermal catastrophe*.

To analyse these results in a more detailed way we need to use the *theory of linear series* by Poincaré. This technique is related to the study of the global stability of the equilibria of a generic system. In many static problems the description of a system depends on some parameter other than the generalized coordinates q_i ($i = 1, \ldots, n$) in terms of which we describe the configuration of a system. If μ is the parameter we are talking about, and U is the potential energy of the system, the condition for the existence of an equilibrium is that the plane tangent to the n-dimensional surface $U(\mu, q_i) = \text{const}$ in the equilibrium point is perpendicular to the μ axis; so we obtain an equilibrium configuration for every fixed value of μ and therefore, if we call q_i^0 this configuration, we have $q_i^0 = q_i^0(\mu)$. These points are called *level points* and by varying the value of the parameter μ they form a curve called *linear series*.

To verify the stability of these equilibria we restrict our attention on a plane $\mu = \text{const}$; in statics the condition for an equilibrium to be stable is that the potential energy U in that point is a minimum. This statement means that a point on a linear series represents a stable configuration only if all the different vertical sections of the surface $U = \text{const}$ across that point are turned towards the direction of decreasing U; it is possible to prove (see, *e.g.*, [3]) that every change in the stability of a system corresponds to an extremum of the linear series.

In a pioneering work, Lynden-Bell and Wood [4] applied this method to investigate the stability of an isotropic isothermal stellar system truncated in radius. In this case the equilibrium states in the presence of encounters are featured by having

$$S = \max \text{ with } \begin{cases} E = \text{const}\,, \\ M = \text{const}\,, \end{cases} \tag{4}$$

where S is the entropy, and E and M are the total energy and the total mass of the system. The distribution function (DF) that describes the system under these requirements is given by the Maxwell-Boltzmann DF

$$f(\varepsilon) = Ae^{-\beta\varepsilon}, \tag{5}$$

where $\varepsilon = v^2/2 + \Phi$ is the energy of a single star composing the system, $\beta = \frac{1}{\kappa T}$, A is a normalization constant and Φ is the self-consistent potential obtained by solving the Poisson equation:

$$\nabla^2 \Phi(r) = -4\pi G\varrho(r) \tag{6}$$

with the density ϱ given by

$$\varrho(r) = \int f(r, v)\, \mathrm{d}^3 v = Be^{\beta\Phi(r)} \tag{7}$$

($B = A(2\pi/\beta)^{3/2}$). Lynden-Bell and Wood were interested into the stability of a system with respect to perturbations keeping constant the total mass M, the total energy E and the radius (or the volume) of the configuration. In this case the entropy $-S$ of the system was the potential energy U, because for such systems S is a maximum for stable

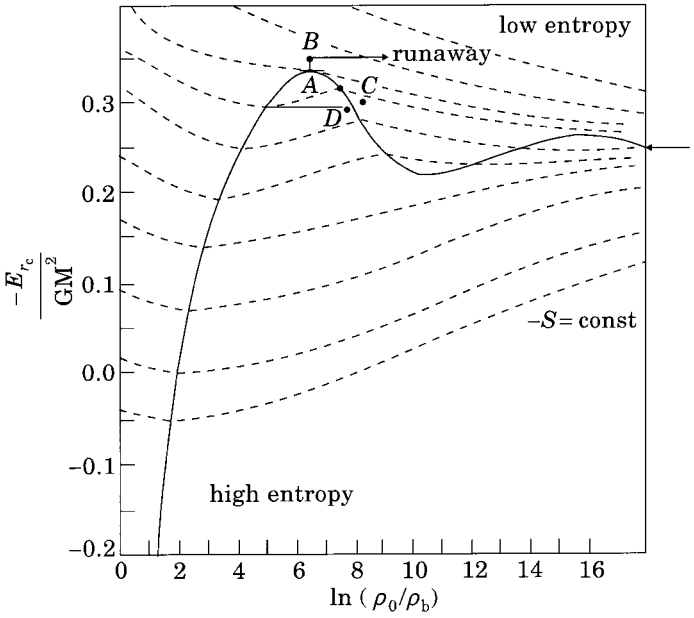

Fig. 1. – Diagram of the energy *vs.* the density contrast in the case of isothermal sphere truncated in radius. The dashed lines are the curves of constant entropy (taken and adapted from Lynden-Bell and Wood [4]).

equilibrium configurations, the density ϱ was the generalised coordinate q_i, and the energy E was the parameter μ because an equilibrium is stable if $-S$ is a minimum for fixed E; all the other quantities were kept fixed.

The results are shown in fig. 1, where the solid line represents the series while the dashed lines are the curves with constant entropy; the equilibria of the system are stable (states featured by a maximum of the entropy) until we reach the maximum of the curve $E = E(\varrho)$; after that maximum we can only have states where the entropy is a minimum, *i.e.* unstable equilibrium configurations. This inversion point corresponds to a density contrast $\frac{\varrho_0}{\varrho_b} = 709$, where ϱ_0 and ϱ_b are the values of the central and of the boundary density. This value is obtained for a critical radius $r_c = 0.335GM^2/(-E)$, in agreement with the qualitative results formerly shown.

Unfortunately, this description was not useful to describe real stellar systems because of the radial cut-off implying a non-zero boundary pressure that allows the system to expand and reach non-physical configurations featured by having infinite radius and mass. More realistic models are obtained by considering energy-truncated distribution functions, *i.e.* Maxwellian distributions where the cut is in the energy of the single star so that all the stars endowed with a velocity higher than the escape velocity are removed from the system. It is possible to find many different distribution functions having this property; the most famous one is the *King distribution* [5]:

$$f_K(\varepsilon) = \frac{A}{(2\pi\sigma^2)^{3/2}}\left(e^{-\frac{\varepsilon}{\sigma^2}} - 1\right) \tag{8}$$

when $\varepsilon < 0$ and zero otherwise. Here A is a new normalization constant and $\sigma^2 = \kappa T$ is the velocity dispersion. Other functions were introduced by Woolley and Dickens [6]:

$$f_{\mathrm{WD}}(\varepsilon) = \frac{A}{(2\pi\sigma^2)^{3/2}} e^{-\varepsilon/\sigma^2}, \tag{9}$$

and by Wilson [7]:

$$f_{\mathrm{W}}(\varepsilon) = \frac{A}{(2\pi\sigma^2)^{3/2}} \left(e^{-\varepsilon/\sigma^2} + \frac{\varepsilon}{\sigma^2} - 1 \right) \tag{10}$$

both for $\varepsilon < 0$, while they are zero otherwise. Note that in all these functions ε is the energy of a star normalized to zero at the boundary of the configuration $r = r_{\mathrm{b}}$:

$$\varepsilon \equiv \frac{v^2}{2} + \Phi(r) - \Phi(r_{\mathrm{b}}) = \frac{v^2}{2} - \Psi(r), \tag{11}$$

where $\Psi(r) \equiv -\Phi(r) + \Phi(r_{\mathrm{b}})$ is the normalized potential.

In his works Katz [8, 9] evaluated the stability with respect to the phenomenon of the gravothermal catastrophe of such more physical models; in this case the study of the stability was carried out for systems with constant mass and energy and in correspondence of fixed normalization parameter A to ensure the local thermodynamic equilibrium. He plotted the total energy E *vs.* the central potential Ψ_{c} because this quantity has the property of being uniquely defined for every chosen configuration when all the other parameters describing the system are kept fixed. Once again the maxima and the minima of the curve are the only places where a change of stability may occur; he found that the systems under consideration reach the conditions for the onset of the instability when the central potential assumes the values

$$\begin{cases} 1)\ \Psi_{\mathrm{c}} = 7.8\sigma^2 & \text{Woolley-Dickens models}, \\ 2)\ \Psi_{\mathrm{c}} = 7.4\sigma^2 & \text{King models}, \\ 3)\ \Psi_{\mathrm{c}} = 6.6\sigma^2 & \text{Wilson models}. \end{cases} \tag{12}$$

2. – Anisotropic models

In this section we study spherical families of models with an anisotropic velocity dispersion, focussing our attention on the role played by the anisotropy on the stability of such systems with respect to the phenomenon of the gravothermal catastrophe.

2˙1. *Description of anisotropic spherical models.* – The importance of an anisotropic model for the description of real spherical stellar systems arises when studying the first periods of life of glubular clusters: it is possible to demonstrate that at the end of the process of the *Violent Relaxation* [10] all the merging systems are anisotropic because they still have stars mainly distributed on radial orbits and although they will tend to relax and become isotropic on a time scale which is of the

order of the relaxation time (see [1]), if the conditions for the onset of the gravothermal instability take place before their total isotropization, we will have to deal with the study of the stability of these systems without leaving the anisotropy out of consideration.

The distribution functions introduced to describe such anisotropic systems are [11]

$$(13)\qquad \begin{cases} 1)\ f_{\mathrm{WD}}(\varepsilon, L^2) = \dfrac{A}{(2\pi\sigma^2)^{3/2}}\, e^{-\frac{\varepsilon}{\sigma^2}}\, e^{-\frac{L^2}{2\sigma^2 r_a^2}}, \\ 2)\ f_{\mathrm{K}}(\varepsilon, L^2) = \dfrac{A}{(2\pi\sigma^2)^{3/2}} \left(e^{-\frac{\varepsilon}{\sigma^2}} - 1\right) e^{-\frac{L^2}{2\sigma^2 r_a^2}}, \\ 3)\ f_{\mathrm{W}}(\varepsilon, L^2) = \dfrac{A}{(2\pi\sigma^2)^{3/2}} \left(e^{-\frac{\varepsilon}{\sigma^2}} + \dfrac{\varepsilon}{\sigma^2} - 1\right) e^{-\frac{L^2}{2\sigma^2 r_a^2}} \end{cases}$$

when $\varepsilon < 0$ and zero otherwise; ε is the energy of the single particle belonging to the system as defined in eq. (11). The dependence of the factor $k(L^2) = e^{-\frac{L^2}{2\sigma^2 r_a^2}}$ on the square of the angular momentum L is to ensure the spherical global properties of the models; r_a is called *anisotropy radius* and it is approximately the value of the radius beyond which the orbits start to be mainly radial.

In order to perform the integration of these models, we define the following dimensionless quantities:

$$(14)\qquad \widetilde{\Psi} = \frac{\Psi}{\sigma^2}, \quad \tilde{\varepsilon} = \frac{\varepsilon}{\sigma^2}, \quad \tilde{v}^2 = \frac{v^2}{\sigma^2}, \quad x = \frac{r}{r_{\mathrm{K}}}, \quad \gamma = \frac{r_a}{r_{\mathrm{K}}},$$

where r_{K}, defined through

$$(15)\qquad r_{\mathrm{K}}^2 = \frac{9\sigma^2}{4\pi G \varrho_{\mathrm{c}}},$$

is called *core radius* or *King radius* and gives the length scale; ϱ_{c} is the central density.

To obtain the characteristic densities we have to integrate the distribution functions (13) over the velocity space

$$(16)\qquad \varrho(\Psi(r), r) = \int f(\varepsilon, L^2)\, \mathrm{d}^3 v.$$

Writing the volume element $\mathrm{d}^3 v$ in spherical coordinates (v, θ, ψ), and introducing the appropriate integration extremes, suitable for the physical situation, we have

$$(17)\qquad \varrho(\Psi(r), r) = 2\pi \int_0^{\sqrt{2\Psi(r)}} v^2\, \mathrm{d}v \int_0^{\pi} f\left(\frac{v^2}{2} - \Psi(r), |rv\sin\theta|\right) \sin\theta\, \mathrm{d}\theta,$$

where we carried out the integration over the ψ angle because of the independence of the distribution functions from this variable. If we show in an explicit way the

dependence of the DF on L^2 we obtain

$$\varrho(\Psi(r),\, r) = 2\pi \int_0^{\sqrt{2\Psi(r)}} g\left(\frac{v^2}{2} - \Psi(r)\right) v^2\, \mathrm{d}v \int_0^{\pi} e^{-\frac{r^2 v^2 \sin^2\theta}{2 r_a^2 \sigma^2}} \sin\theta\, \mathrm{d}\theta\,, \tag{18}$$

where $g(v^2/2 - \Psi(r))$ can be whatever distribution function among those in eqs. (8), (9), (10). By introducing the new variable $\chi = \dfrac{rv}{\sqrt{2} r_a \sigma} = \dfrac{x\tilde{v}}{\sqrt{2\gamma}}$, the integral on the right side of (18) takes the new form

$$\int_0^{\pi} e^{-\frac{x^2 \tilde{v}^2 \sin^2\theta}{2\gamma^2}} = \frac{2}{\chi}\mathscr{D}(\chi) \tag{19}$$

with $\mathscr{D}(\chi)$ the *Dawson function* defined as

$$\mathscr{D}(\chi) \equiv e^{-\chi^2} \int_0^{\chi} e^{t^2}\, \mathrm{d}t\,.$$

If we insert eq. (19) in (18) and write the proper expressions (8), (9), (10) instead of $g(\varepsilon)$, we finally have the anisotropic-model densities:

$$\begin{cases} 1)\ \varrho_{\mathrm{WD}}(\widetilde{\Psi}(x),\, x) = \dfrac{4A}{\sqrt{\pi}}\,\dfrac{\gamma}{x}\, e^{\widetilde{\Psi}(x)} \displaystyle\int_0^{\sqrt{\widetilde{\Psi}(x)}} e^{-t^2} t \mathscr{D}\left(\frac{xt}{\gamma}\right) \mathrm{d}t\,, \\ 2)\ \varrho_{\mathrm{K}}(\widetilde{\Psi}(x),\, x) = \dfrac{4A}{\sqrt{\pi}}\,\dfrac{\gamma}{x} \displaystyle\int_0^{\sqrt{\widetilde{\Psi}(x)}} (e^{\widetilde{\Psi}(x)} e^{-t^2} - 1)\, t \mathscr{D}\left(\frac{xt}{\gamma}\right) \mathrm{d}t\,, \\ 3)\ \varrho_{\mathrm{W}}(\widetilde{\Psi}(x),\, x) = \dfrac{4A}{\sqrt{\pi}}\,\dfrac{\gamma}{x} \displaystyle\int_0^{\sqrt{\widetilde{\Psi}(x)}} (e^{\widetilde{\Psi}(x)} e^{-t^2} - \widetilde{\Psi}(x) + t^2 - 1)\, t \mathscr{D}\left(\frac{xt}{\gamma}\right) \mathrm{d}t\,, \end{cases} \tag{20}$$

where $t = \dfrac{\tilde{v}}{\sqrt{2}}$. Note that the density values in the presence of anisotropy depend on the radial coordinate r both directly and in an implicit way through the potential $\Psi(r)$, contrary to what happens when considering the corresponding isotropic ones where the dependence is only through $\Psi(r)$.

As we have seen, the self-consistent potential $\Psi(r) = -\Phi(r) + \Phi(r_b)$, where Φ is the "real" potential, is obtained by solving the Poisson equation (6). If we make all the quantities in that equation dimensionless by using the expressions in (14), then we obtain

$$\frac{1}{x^2}\,\frac{\mathrm{d}}{\mathrm{d}x}\left(x^2\,\frac{\mathrm{d}\widetilde{\Psi}}{\mathrm{d}x}\right) = \frac{\mathrm{d}^2\widetilde{\Psi}}{\mathrm{d}x^2} + \frac{2}{x}\,\frac{\mathrm{d}\widetilde{\Psi}}{\mathrm{d}x} = \frac{4\pi G r_K^2}{\sigma^2} = -9\,\frac{\varrho(\widetilde{\Psi}(x),\, x)}{\varrho_c}\,, \tag{21}$$

where the last equation comes from the substitution of r_K with its explicit expression.

We can now solve Cauchy's problem with initial conditions

$$\begin{cases} \widetilde{\Psi}(0) = \widetilde{\Psi}_c, \\ \widetilde{\Psi}'(0) = 0 . \end{cases} \tag{22}$$

We carried out the integration of the anisotropic Woolley-Dickens, King and Wilson models by selecting different values of the anisotropy parameter γ and of the central potential Ψ_c; γ was chosen so that we could range from almost isotropic configurations ($\gamma = 100$) up to configurations where the anisotropy enters the core ($\gamma = 0.3$), with Ψ_c varying from a minimum value of $0.2\sigma^2$ up to $10\sigma^2$.

The first, very interesting feature met while analysing these models is the existence of a definite couple of values (γ, Ψ_c) that identify infinite models, *i.e.* models endowed with an infinite tidal radius; more in detail, there is a critical value of the central potential, depending on the degree of anisotropy that chacterises every model, beyond which we have $r_b \to \infty$ for every γ. This happens even though the distribution functions used for the description of these models are energy-truncated, and the corresponding isotropic configurations are always bounded; this remarkable peculiarity is common to all the anisotropic models independently of the functions (13).

In figs. 2, 3, 4 we have plotted the central potential Ψ_c as a function of the quantity γ_{BS} for the anisotropic Woolley-Dickens, King and Wilson models, respectively. Every plot shows a monoparametric sequence corresponding to the first unbounded models of equilibrium on the plane (Ψ_c, γ_{BS}): every point on the diagram determines in a unique way the first model of equilibrium endowed with an infinite radius. The quantity γ_{BS} has been introduced to compare our results with those obtained by Stiavelli-

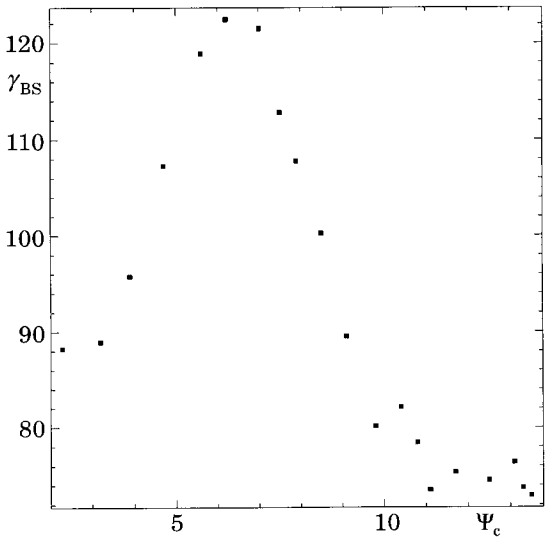

Fig. 2. – Central potential Ψ_c, measured by units of σ^2, as a function of the anisotropy parameter γ_{BS} in correspondence of the first unbounded models resulting from the anisotropic Woolley-Dickens distribution function.

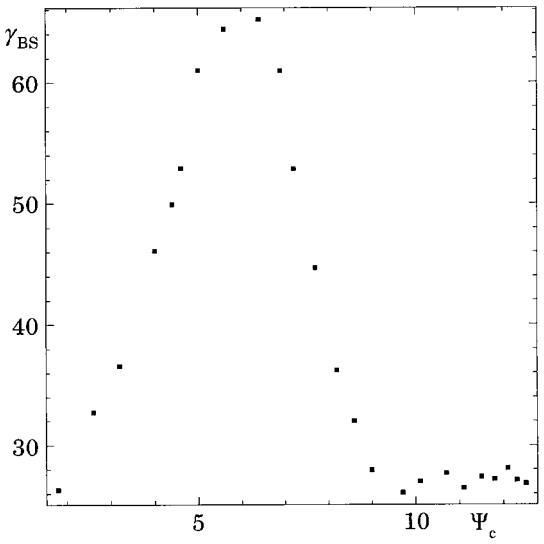

Fig. 3. – Central potential Ψ_c, measured by units of σ^2, as a function of the anisotropy parameter γ_{BS} in correspondence of the first unbounded models resulting from the anisotropic King distribution function.

Bertin [12, 13] during the study of their models, and is related to our γ through the relation

$$\gamma_{BS} \propto \frac{\varrho_c}{\gamma^2} . \tag{23}$$

In fig. 5 we show the trend of the Stiavelli-Bertin monoparametric family of models on the same plane (Ψ_c, γ_{BS}); it is evident that this trend is the same as obtained in the former diagrams, with a prominent maximum followed by a number of oscillations featured by local maxima and minima of lower amplitude. Therefore we can conclude that *such behaviour is common to all the spherical anisotropic models having a dependence on the angular momentum of the kind* e^{-L^2}*, regardless of the form of the energy distribution.* A remarkable thing to note is that not all these models represent real physical systems; if we try to to write for each one of them the dimensionless mass $\tilde{m}$ defined as

$$\tilde{m} = 4\pi \int_0^\infty \frac{\varrho(\tilde{\Psi}(x), x)}{\varrho_c} x^2 \, dx , \tag{24}$$

where we used the quantities introduced in (14), we find that this value is definite and smaller than infinity only when considering anisotropic Wilson and Stiavelli-Bertin models, while it is equal to infinity for anisotropic Woolley and King models. This means that the former models, although having an infinite tidal radius, can describe real stellar systems because of the properties of their mass, while the second ones cannot have any physical meaning.

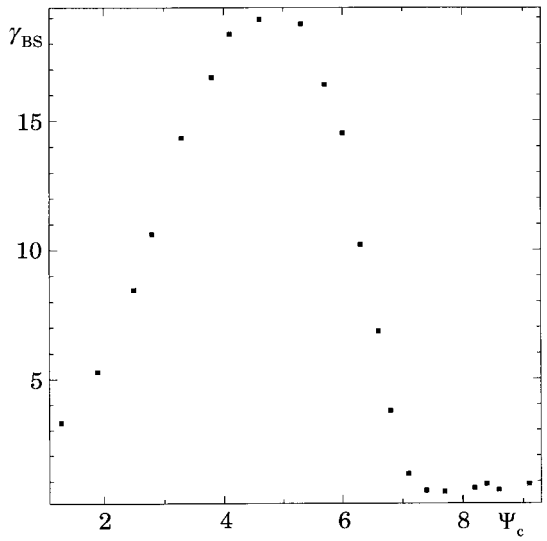

Fig. 4. – Central potential Ψ_c, measured by units of σ^2, as a function of the anisotropy parameter γ_{BS} in correspondence of the first unbounded models resulting from the anisotropic Wilson distribution function.

2'2. *Gravothermal instability of spherical anisotropic models.* – The aim of this section is to evaluate the conditions for the onset of the gravothermal instability in the case of anisotropic spherical systems. The investigation has been carried out by means of the method of the linear series; because of the dependence of the distribution functions (13) on the three parameters A, σ, γ (or r_a) and on the central potential Ψ_c, we will have to fix, in agreement with the theory,

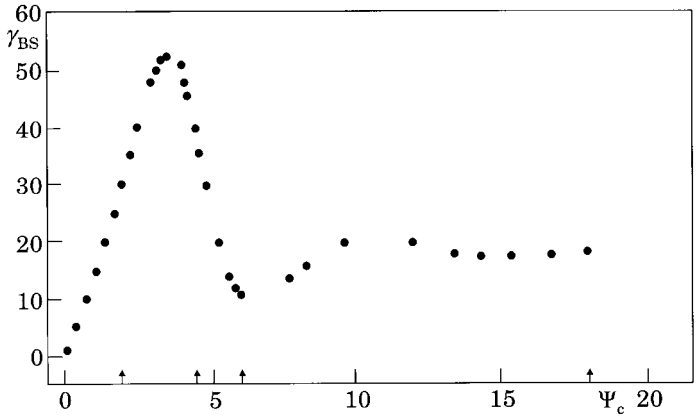

Fig. 5. – Monoparametric family of spherical Stiavelli-Bertin equilibrium configurations. On the y-axis the parameter γ_{BS} is plotted as a function of the central potential Ψ_c measured by units of σ^2 (from [13]).

three quantities belonging to the particular model under consideration and let a fourth quantity vary as a function of a parameter that is able to describe such model in a unique way.

Considering the densities (20) and writing down their values in the centre of the configurations, we obtain

$$(25)\qquad \begin{cases} 1)\ \varrho_{\mathrm{WD}}(0) = \dfrac{4A}{\sqrt{\pi}}\, e^{\tilde{\Psi}(0)} \displaystyle\int_0^{\sqrt{\tilde{\Psi}(0)}} e^{-t^2} t^2\, \mathrm{d}t\,, \\ 2)\ \varrho_{\mathrm{K}}(0) = \dfrac{4A}{\sqrt{\pi}} \displaystyle\int_0^{\sqrt{\tilde{\Psi}(0)}} [e^{\tilde{\Psi}(0)} e^{-t^2} - 1]\, t^2\, \mathrm{d}t\,, \\ 3)\ \varrho_{\mathrm{W}}(0) = \dfrac{4A}{\sqrt{\pi}} \displaystyle\int_0^{\sqrt{\tilde{\Psi}(0)}} [e^{\tilde{\Psi}(0)} e^{-t^2} + t^2 - \tilde{\Psi}(0) - 1]\, t^2\, \mathrm{d}t\,. \end{cases}$$

Starting from the dimensionless Poisson equation (21), it is possible to obtain the value of the total mass for the anisotropic systems by integration of both members of this equation between 0 and the dimensionless tidal radius $x_{\mathrm{T}} = r_{\mathrm{b}}/r_{\mathrm{K}}$; the resulting expression for the total dimensionless mass is given by

$$(26)\qquad \tilde{m} = -\frac{4\pi}{9} x^2 \frac{\mathrm{d}\tilde{\Psi}}{\mathrm{d}x}\,\Big|_{(x = x_{\mathrm{T}})}.$$

The total energy E can be calculated in the same way by definition of the dimensionless potential energy w:

$$(27)\qquad w = 4\pi \int_0^{x_{\mathrm{T}}} \frac{\varrho(x)}{\varrho_{\mathrm{c}}}\, \tilde{\Psi}(x) x^2\, \mathrm{d}x\,,$$

where ϱ_{c} can be whatever expression from those in (25). Using the virial theorem in the absence of boundary pressure we obtain

$$(28)\qquad E = \frac{U}{2} = \frac{1}{2} \int_0^{r_{\mathrm{T}}} 4\pi\varrho(r)\, \Phi(r)\, r^2\, \mathrm{d}r\,.$$

By introduction of the scaled potential Ψ, and using once more the dimensionless quantities (14) we have

$$(29)\qquad E = \frac{1}{2}\varrho_{\mathrm{c}} r_{\mathrm{K}}^3 \sigma^2 \int_0^{x_{\mathrm{T}}} 4\pi(-\tilde{\Psi}(x)) \frac{\varrho(x)}{\varrho_{\mathrm{c}}} x^2\, \mathrm{d}x - \frac{GM^2}{2r_{\mathrm{b}}} = -\frac{1}{2}\varrho_{\mathrm{c}} r_{\mathrm{K}}^2 \sigma^2 w - \frac{GM^2}{2r_{\mathrm{b}}}\,,$$

where we used the expression (27) to write the last equality. Therefore, the total

energy of the system takes the form

$$E = -\frac{GM^2}{r_b}\left(\frac{2\pi}{9}\,\frac{wx_T}{\tilde{m}} + \frac{1}{2}\right). \tag{30}$$

In order to apply the theory of linear series to study the stability of these systems, because of the dependence of the distribution functions (13) on four parameters, we have to fix three quantities involved in the description of the model so that all the other quantities will depend only on a fourth parameter that will be chosen to characterize in a unique way the equilibrium sequences.

We decided to keep fixed on every sequence the normalization constant A, the total (dimensional) mass of the system M, and the anisotropy parameter γ; the choice of fixing A is due to the necessity of ensuring the local thermodynamic equilibrium inside the configuration by means of the *Gibbs-Duhem equation* [9]:

$$N\,\mathrm{d}\omega + S\,\mathrm{d}T + V\,\mathrm{d}P = 0\,, \qquad \forall r\,, \tag{31}$$

where N is the number of stars belonging to the system, ω is the chemical potential that is shown to be the boundary gravitational potential Φ_b [14], S is the entropy, T is the temperature, V is the volume and P is the pressure, and where all these quantities are evaluated in every single shell $(r, r + \mathrm{d}r)$.

The constancy of the mass M is justified by the fact that the kind of systems we are considering is closed and therefore the process of gravothermal instability will happen in the absence of evaporation, *i.e.* it is a constant-mass process. The parameter γ has been held constant because we are not interested in time evolution, evolution that leads to a variation of the degree of anisotropy inside the configuration [15], but we are only searching for the conditions for the models to become unstable: so we choose to fix a quantity which could give the amount of anisotropy globally present in the system when the instability begins. Anyway, it is worthy to note that the anisotropy parameter is only one of the possible choices because we can always find other quantities related to the anisotropy of the configurations that could be held constant along the equilibrium sequences.

We put in arbitrary units:

$$A = 1\,, \qquad M = 1\,, \qquad G = \frac{1}{4\pi} \tag{32}$$

and by introduction of the right expressions for the quantities in the definition of the mass $M = \varrho_c r_c^3 \tilde{m} = 1$, we found

$$\sigma = \left(\frac{2\pi}{81}\right)^{1/2}\left(\frac{\varrho_c}{\tilde{m}^2}\right)^{1/3}. \tag{33}$$

Therefore, if we insert (32) and (33) in the expression for the total energy, we finally obtain

$$E = -\frac{1}{2x_T}\,\frac{\varrho_c^{2/3}}{9\,\tilde{m}^{1/3}}\left(\frac{2\pi w x_T}{9\,\tilde{m}^2} + \frac{1}{2}\right). \tag{34}$$

We can now determine the stability of our models with respect to perturbations keeping fixed the values of the mass, of the anisotropy parameter and of A in the case

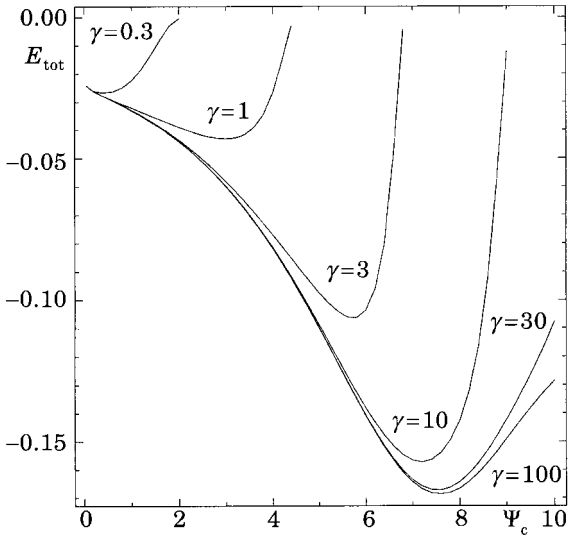

Fig. 6. – Analysis of the stability of anisotropic Woolley-Dickens models as a function of the anisotropy parameter γ.

of anisotropic Woolley-Dickens, King and Wilson models; the dimensionless central potential $\widetilde{\Psi}_c$ has been chosen as the independent variable to describe the whole system and therefore the total energy will be a function only of that quantity (for A, γ and M held constant). In figs. 5, 6, 7 we plotted the total energy E *vs.* $\widetilde{\Psi}_c$ for different values of γ: every curve is a linear series describing a set of models having the same values of M,

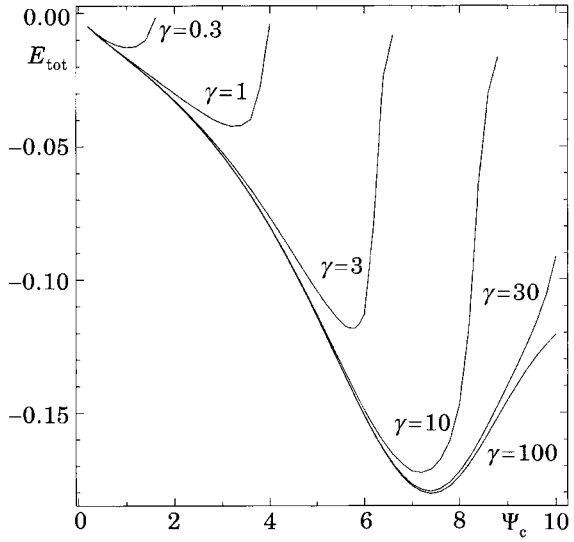

Fig. 7. – Analysis of the stability of anisotropic King models as a function of the anisotropy parameter γ.

A and γ. The quantity γ varies through a wide range of values and it has been used to parameterize the sequences; more in detail, the value $\gamma = 100$ corresponds to an isotropic model (radial anisotropy starting from $r \simeq 100\, r_{\mathrm{K}}$), while $\gamma = 0.3$ is for almost completely anisotropic model (anisotropy inside the nucleus for $r \simeq 0.3 r_{\mathrm{K}}$).

The minima of these curves show the configurations in correspondence of which we have the transition between stable and unstable models; the portion of the curves on the left-hand side of the minima represents configurations that result to be stable, while the ones on the right-hand side undergo the process of gravothermal instability. As is possible to notice, all the diagrams have the same trend, without any regard to the the fact that the models were anisotropic Woolley, King or Wilson ones: for values of the anisotropy parameter $\gamma \geqslant 30$ the critical value of the central potential that determines the onset of the instability is the same as for the isotropic case (see, *e.g.*, [9]); this is expected if one considers that for large values of γ only the very outer regions of the systems are affected by the presence of anisotropy. When anisotropy enters the system (smaller values of γ) there is a significant shift of the minima towards the left-hand side of the diagram, the closer to the nucleus the anisotropy starts, the more this shift is marked. This behaviour implies that, with the prevalence of radial orbits inside the models, the corresponding configurations loose their stability "earlier", where the word earlier stands for smaller central potentials and smaller tidal energies, *i.e.* for fields acting on the components of the systems which result to be weaker.

3. – Comparison between radial and gravothermal instability

A phenomenon which must have been taken into account while studying the stability of anisotropic spherical systems is the *radial-orbit instability*, so called because of its occurrence in models with predominantly radial orbits. This instability is due to the fact that approximately radial orbits are almost closed (angle between successives apocenters $\Delta\varphi \simeq \pi$), thus non-radial forces acting on them can in some cases realign their orientation, leading to a distortion of the whole system into a triaxial configuration [16]. Numerical simulations have shown that when the amount of anisotropy in a spherical stellar system is greater than a threshold value, its evolution is always towards a final state featured by having a triaxial symmetry or a barlike shape (see, *e.g.*, [17]). Therefore, after the discussion of the stability of anisotropic spherical configurations with respect to the process of gravothermal catastrophe, the next step in the study of such systems is to verify if gravothermally stable models are also dynamically stable when considering the phenomenon of radial-orbit instability; this request arises since endowing models with an anisotropic velocity distribution, *i.e.* making radial orbits more populated than the tangential ones, may cause the onset of this last phenomenon, that should lead to a modification of the structure of the whole system from its original shape, before the collapse of the core due to the process of gravothermal instability starts, thus invalidating all the results formerly obtained in the case of spherical configurations.

We choose the quantity $2K_{\mathrm{R}}/K_{\mathrm{T}}$, with K_{R} and K_{T} total radial and tangential kinetic energy, as the "parameter" to evaluate the radial instability of the systems under consideration; this choice comes from a great amount of numerical simulations [18, 19] that have shown how the onset of this process is related to the achievement of a threshold value of $2K_{\mathrm{R}}/K_{\mathrm{T}}$ that lies approximately between 1.5 and 1.8.

To evaluate this ratio we need to know the values of the radial and of the tangential energy, whose expressions are given by

$$K_{\mathrm{R}} = \frac{1}{2}\int_0^{r_{\mathrm{T}}} 4\pi r^2 \varrho(r)\langle v_{\mathrm{R}}^2(r)\rangle \,\mathrm{d}r\,, \tag{35}$$

$$K_{\mathrm{T}} = \frac{1}{2}\int_0^{r_{\mathrm{T}}} 4\pi r^2 \varrho(r)\langle v_{\mathrm{T}}^2(r)\rangle \,\mathrm{d}r\,, \tag{36}$$

where $\varrho(r)$ can be whatever density coming from an anisotropic Woolley, King or Wilson description; $\langle v_{\mathrm{R}}^2\rangle$ and $\langle v_{\mathrm{T}}^2\rangle$ are the mean-square values of the radial and the tangential components of the velocity of a single star composing the system, with

$$\langle v_{\mathrm{R}}^2(r)\rangle = \frac{2\pi}{\varrho(r)}\int_0^{\sqrt{2\Psi(r)}} v^4 g\left(\Psi(r) - \frac{1}{2}v^2\right)\mathrm{d}v \int_0^{\pi} \sin\theta\cos^2\theta e^{-v^2 r^2 \sin^2\theta/2\sigma^2 r_{\mathrm{a}}^2}\,\mathrm{d}\theta \tag{37}$$

and

$$\langle v_{\mathrm{T}}^2(r)\rangle = \langle v^2(r)\rangle - \langle v_{\mathrm{R}}^2(r)\rangle, \tag{38}$$

where

$$\langle v^2(r)\rangle = \frac{2\pi}{\varrho(r)}\int_0^{\sqrt{2\Psi(r)}} v^4 g\left(\Psi(r) - \frac{1}{2}v^2\right)\mathrm{d}v \int_0^{\pi} \sin\theta e^{-v^2 r^2 \sin^2\theta/2\sigma^2 r_{\mathrm{a}}^2}\,\mathrm{d}\theta \tag{39}$$

and where $g(\Psi - \frac{1}{2}v^2)$ can be whatever distribution function (8), (9) or (10). Using the expressions in (14), and putting

$$g\left(\Psi - \frac{1}{2}v^2\right) = \frac{A}{(2\pi\sigma^2)^{3/2}}\tilde{g}\left(\Psi - \frac{1}{2}v^2\right), \qquad \varrho = A\tilde{\varrho}\,, \qquad t^2 = \frac{\tilde{v}^2}{2}\,,$$

after some calculations we have

$$\langle v_{\mathrm{R}}^2(x)\rangle = \frac{1}{\tilde{\varrho}(x)}\,\frac{4}{\sqrt{\pi}}\,\sigma^2\left(\frac{\gamma}{x}\right)^3 \int_0^{\sqrt{\tilde{\Psi}(x)}} t\tilde{g}(\tilde{\Psi}(x) - t^2)\left[\frac{tx}{\gamma} - \mathscr{D}\left(\frac{tx}{\gamma}\right)\right]\mathrm{d}t\,, \tag{40}$$

$$\langle v_{\mathrm{T}}^2(x)\rangle = \frac{1}{\tilde{\varrho}(x)}\,\frac{8}{\sqrt{\pi}}\,\sigma^2\left(\frac{\gamma}{x}\right) \int_0^{\sqrt{\tilde{\Psi}(x)}} t^3\tilde{g}(\tilde{\Psi}(x) - t^2)\,\mathscr{D}\left(\frac{tx}{\gamma}\right)\mathrm{d}t - \langle v_{\mathrm{R}}^2\rangle, \tag{41}$$

where $\mathscr{D}(\frac{tx}{\gamma})$ is the Dawson function. By inserting these two last equations into (35) and (36), and by using once again the dimensionless quantities introduced in (14), we

finally obtain

$$K_{\mathrm{R}} = \frac{1}{2}\varrho_{\mathrm{c}} r_{\mathrm{c}}^3 \sigma^2 \int_0^{x_{\mathrm{T}}} \frac{4\pi x^2}{\tilde{\varrho}_{\mathrm{c}}} \left\{ \frac{4}{\sqrt{\pi}} \left(\frac{\gamma}{x} \right)^3 \int_0^{\sqrt{\tilde{\Psi}(x)}} t \tilde{g}(\tilde{\Psi}(x) - t^2) \left[\frac{tx}{\gamma} - \mathscr{D}\left(\frac{tx}{\gamma} \right) \right] \mathrm{d}t \right\} \tag{42}$$

and

$$K_{\mathrm{T}} = \frac{1}{2}\varrho_{\mathrm{c}} r_{\mathrm{c}}^3 \sigma^2 \int_0^{x_{\mathrm{T}}} \frac{4\pi x^2}{\tilde{\varrho}_{\mathrm{c}}} \left\{ \frac{8}{\sqrt{\pi}} \left(\frac{\gamma}{x} \right) \int_0^{\sqrt{\tilde{\Psi}(x)}} t^3 \tilde{g}(\tilde{\Psi}(x) - t^2) \, \mathscr{D}\left(\frac{tx}{\gamma} \right) \mathrm{d}t - \langle v_{\mathrm{R}}^2 \rangle \right\}. \tag{43}$$

We can now perform the numerical integration of the quantity $2K_{\mathrm{R}}/K_{\mathrm{T}}$, being careful attention in the neigbourhood of the origin because in the limit $r/r_{\mathrm{K}} \ll 1$ the values of (42) and (43) were not well defined, so it had been necessary to consider the development of the K_{R} and K_{T} expressions for $x \to 0$, obtaining the same values as in the case of isotropic models. Such developments have been performed for radii up to the value of $x \simeq 10^{-1}$, with a variability depending on the degree of anisotropy that featured each model: the more the system resembled an isotropic one (anisotropy starting from greater radii), the wider was the region inside the nucleus where this development has been used. We chose $2K_{\mathrm{R}}/K_{\mathrm{T}} = 1.7$ as the threshold value for the onset of the radial-orbit instability, in agreement with the results found by Fridman and Polyachenko. Our results and the following comparison between the gravothermal and the radial instability are shown in figs. 9, 10 and 11: here we plotted the behaviour of $2K_{\mathrm{R}}/K_{\mathrm{T}}$ as a function of the dimensionless central potential $\tilde{\Psi}_{\mathrm{c}}$ in the case of anisotropic Woolley-Dickens, King and Wilson models, and for different values of the anisotropy

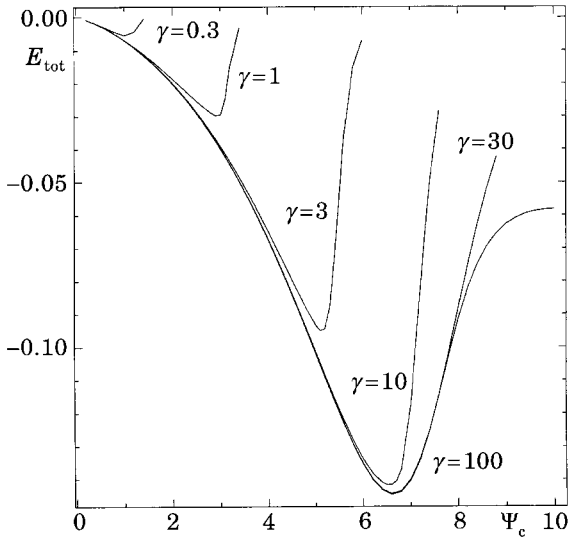

Fig. 8. – Analysis of the stability of anisotropic Wilson models as a function of the anisotropy parameter γ.

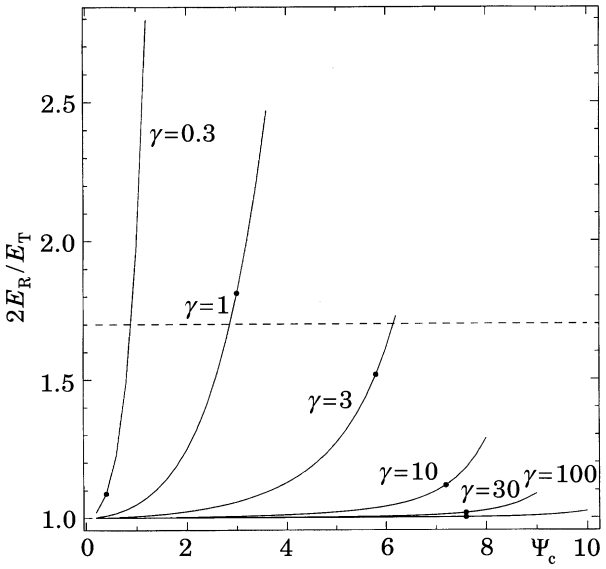

Fig. 9. – Behaviour of the quantity $2K_R/K_T$ as a function of the central potential in the case of anisotropic Woolley-Dickens models and for different values of γ; the black dots individuate the first configurations gravothermally unstable, while the dashed line is the threshold value for the onset of the radial instability.

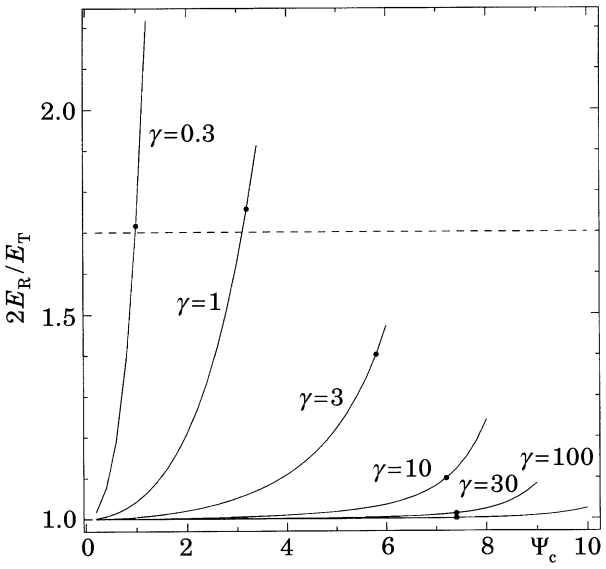

Fig. 10. – Behaviour of the quantity $2K_R/K_T$ as a function of the central potential in the case of anisotropic King models and for different values of γ; the black dots individuate the first configurations gravothermally unstable, while the dashed line is the threshold value for the onset of the radial instability.

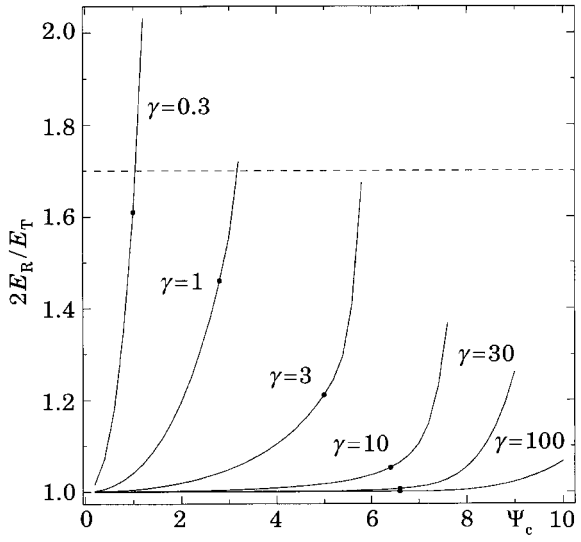

Fig. 11. – Behaviour of the quantity $2K_R/K_T$ as a function of the central potential in the case of anisotropic Wilson models and for different values of γ; the black dots individuate the first configurations gravothermally unstable, while the dashed line is the threshold value for the onset of the radial instability.

parameter γ; the black dots individuate the first gravothermally unstable configurations (onset of the gravothermal instability, corresponding to the minima in figs. 6, 7 and 8), while the dashed line shows the threshold value for the onset of the dynamical instability. If the amount of anisotropy is not so relevant ($\gamma \gtrsim 3$), all the systems undergo the gravothermal collapse well before being radially unstable (dots under the threshold), while as soon as it grows and enters into the nucleus ($\gamma \lesssim 1$) these two phenomena are almost concomitant, *i.e.* the conditions for one of the instabilities to start are the same that lead to the onset of the other one; if we analyse more in detail all the diagrams, it is possible to see that in the case of Woolley models the configuration featured by having $\gamma = 1$ is radially unstable before being gravothermally unstable, and in the case of King models this sequence of processes happens in both the configurations with $\gamma < 1$. This phenomenon does not appear during the

TABLE I. – *Woolley-Dickens models: critical values of the central potential $\widetilde{\Psi}_c$ as determined by the anisotropy parameter γ.*

	Gravothermal instability	Radial instability	Infinite models
$\gamma = 100$	$\widetilde{\Psi}_c = 7.6$	$\widetilde{\Psi}_c > 10.$	$\widetilde{\Psi}_c = 13.5$
$\gamma = 30$	$\widetilde{\Psi}_c = 7.6$	$\widetilde{\Psi}_c > 10.$	$\widetilde{\Psi}_c = 11.1$
$\gamma = 10$	$\widetilde{\Psi}_c = 7.2$	$\widetilde{\Psi}_c > 8.$	$\widetilde{\Psi}_c = 9.1$
$\gamma = 3$	$\widetilde{\Psi}_c = 5.8$	$\widetilde{\Psi}_c = 6.2$	$\widetilde{\Psi}_c = 7.1$
$\gamma = 1$	$\widetilde{\Psi}_c = 3.$	$\widetilde{\Psi}_c = 2.9$	$\widetilde{\Psi}_c = 4.7$
$\gamma = 0.3$	$\widetilde{\Psi}_c = 0.4$	$\widetilde{\Psi}_c = 0.9$	$\widetilde{\Psi}_c = 2.4$

Table II. – *King models*: *critical values of the central potential* $\widetilde{\Psi}_c$ *as determined by the anisotropy parameter* γ.

	Gravothermal instability	Radial instability	Infinite models
$\gamma = 100$	$\widetilde{\Psi}_c = 7.4$	$\widetilde{\Psi}_c > 10.$	$\widetilde{\Psi}_c = 12.5$
$\gamma = 30$	$\widetilde{\Psi}_c = 7.4$	$\widetilde{\Psi}_c > 10.$	$\widetilde{\Psi}_c = 10.1$
$\gamma = 10$	$\widetilde{\Psi}_c = 7.2$	$\widetilde{\Psi}_c > 8.$	$\widetilde{\Psi}_c = 8.2$
$\gamma = 3$	$\widetilde{\Psi}_c = 5.8$	$\widetilde{\Psi}_c > 6.$	$\widetilde{\Psi}_c = 6.4$
$\gamma = 1$	$\widetilde{\Psi}_c = 3.2$	$\widetilde{\Psi}_c = 3.2$	$\widetilde{\Psi}_c = 4.$
$\gamma = 0.3$	$\widetilde{\Psi}_c = 1.$	$\widetilde{\Psi}_c = 1.$	$\widetilde{\Psi}_c = 1.7$

TABLE III. – *Wilson models: critical values of the central potential* $\widetilde{\Psi}_c$ *as determined by the anisotropy parameter* γ.

	Gravothermal instability	Radial instability	Infinite models
$\gamma = 100$	$\widetilde{\Psi}_c = 6.6$	$\widetilde{\Psi}_c > 10.$	$\widetilde{\Psi}_c = 9.5$
$\gamma = 30$	$\widetilde{\Psi}_c = 6.6$	$\widetilde{\Psi}_c = 9.6$	$\widetilde{\Psi}_c = 7.1$
$\gamma = 10$	$\widetilde{\Psi}_c = 7.5$	$\widetilde{\Psi}_c = 7.9$	$\widetilde{\Psi}_c = 6.6$
$\gamma = 3$	$\widetilde{\Psi}_c = 5.1$	$\widetilde{\Psi}_c = 5.8$	$\widetilde{\Psi}_c = 5.3$
$\gamma = 1$	$\widetilde{\Psi}_c = 2.9$	$\widetilde{\Psi}_c = 3.$	$\widetilde{\Psi}_c = 3.3$
$\gamma = 0.3$	$\widetilde{\Psi}_c = 1.$	$\widetilde{\Psi}_c = 1.$	$\widetilde{\Psi}_c = 1.3$

study of Wilson models that always result to be gravothermally unstable before loosing dynamical stability.

As a matter of fact, for small values of γ, the sequence of processes formerly stated is not as marked as we have shown, because the dots that correspond to the onset of the gravothermal collapse are very close to the dashed line, so if we consider that the value of 1.7 gives us only an estimate of the real critical parameter that lies among a wide range of values, each one strictly depending on the tecnique used for its evaluation, we can conclude that for such models these two instabilities start approximately togheter.

To summarize all the results, in this section we include some tables showing the critical values of the dimensionless central potential and of the anisotropy parameter that determine the onset of the gravothermal instability, the onset of the radial-orbit instability and the first infinite models. (See tables I-III.)

4. – Conclusions

A preliminary analysis of the results obtained suggests that, referring to the onset value for the gravothermal catastrophe, the introduction of a quite high radial anisotropy tends to favour the process, shifting the value of the critical central potential towards lower values. At the same time this increase of anisotropy does not affect the spherical shape and the global properties of such systems unless it happens to be very strong, and therefore, in reasonable low anisotropy limits, the process of

radial-orbit instability does not interfere with the phenomenon of gravothermal collapse. These conclusions must be verified in the framework of a more rigorous analysis and, if confirmed, could well have consequences in the theory of the secular evolution of spherical stellar systems like globular clusters or spherical galaxies.

REFERENCES

[1] BINNEY J. and TREMAINE S., *Galactic Dynamics* (Princeton University Press) 1987.
[2] ANTONOV V. A., *Vest. Leningr. Univ.*, **7** (1962) 135.
[3] JEANS J. H., *Astronomy and Cosmogony* (Cambridge University Press) 1928.
[4] LYNDEN-BELL D. and WOOD R., *Mon. Not. R. Astron. Soc.*, **138** (1968) 495.
[5] KING I. R., *Astron. J.*, **70** (1965) 376.
[6] WOOLLEY R. and DICKENS R. J., *Royal Greenwich Obs. Bulletin*, No. **42**, 1961.
[7] WILSON C. P., *Astron. J.*, **80** (1975) 175.
[8] KATZ J., *Mon. Not. R. Astron. Soc.*, **183** (1978) 765.
[9] KATZ J., *Mon. Not. R. Astron. Soc.*, **190** (1980) 497.
[10] LYNDEN-BELL D., *Mon. Not. R. Astron. Soc.*, **136** (1967) 101.
[11] MICHIE R. W., *Mon. Not. R. Astron. Soc.*, **125** (1963) 127.
[12] STIAVELLI M. and BERTIN G., *Astron. Astrophys.*, **137** (1984) 26.
[13] STIAVELLI M. and BERTIN G., *Mon. Not. R. Astron. Soc.*, **217** (1985) 735.
[14] PADMANABHAN T., *Phys. Rep.*, **188** (1990) 285.
[15] SPURZEM R. and TAKAHASHI K., *Mon. Not. R. Astron. Soc.*, **272** (1995) 772.
[16] PALMER P. L. and PAPALOIZOU J., *Mon. Not. R. Astron. Soc.*, **224** (1987) 1043.
[17] HENON M., *Astron. Astrophys.*, **24** (1973) 229.
[18] MERRITT D., *Astrophys. J.*, **276** (1984) 26.
[19] FRIDMAN A. M. and POLYACHENKO V. L., *Physics of Gravitating Systems* (Springer, New York, N.Y.) 1984.